

## Perovskite Thin Film Preparation and Energy Band-Gap Determination for Solar Cell Applications

Dr. Thaira Z. Altayyar 

Electrical Engineering Department, University of Technology/Baghdad

Email: dr.tyra.uot@hotmail.com

Dr. Shubhra Gangopadhyay

Electrical and Computer Engineering, University of Missouri, Columbia, Missouri, USA

Email: angopadhyays@missouri.edu

Received on:9/3/2016 & Accepted on:19/7/2016

### ABSTRACT:

Using Perovskite is a promising approach for upgrading the performance of an established low-bandgap Si photo voltaic (PV) solar technology because Perovskite is a high bandgap polycrystalline semiconductor compared with bulk Si and other semiconductors such as GaAs. In this work, Perovskite-structured methyl ammonium lead triiodide  $\text{CH}_3\text{NH}_3\text{PbI}_3$  uniform one-step planar thin films nanoparticles (NPs) have been developed from the reaction process of methylammonium iodide with  $\text{PbI}_2$  and deposited on a glass substrate by Aerosol Assisted Chemical Vapor Deposition (AACVD) to minimize the size of the solar cell and to reduce the cost and increase efficiency. This aims at the study and investigation of the energy bandgap ( $E_g$ ) of nano-architected solar cells absorber film as light harvesters. The X-ray diffraction (XRD) patterns of a  $\text{CH}_3\text{NH}_3\text{PbI}_3$  film on glass substrates are recorded by X' Pert Ultima IV X-ray diffractometer. Optical band gap of  $\text{CH}_3\text{NH}_3\text{PbI}_3$  is estimated by UV-Vis absorption spectroscopy and extracted from the absorption spectrum of the Tauc plot to be 1.63 eV. The Perovskite deposited on glass appears efficient to absorb most of the light with wavelength below 800 nm with a refractive index ( $n$ ): 2.75. The film thickness was measured by an optical profile-meter to be about 200 nm, giving small reflectivity of 0.23 and resulting in efficiency enhancement of 15.7 %.

**Keywords:** absorption; bandgap; Perovskite; solar cells.

### INTRODUCTION

Solid-state dye-sensitized solar cells (DSSCs) and, more recently, Perovskite-absorber solar cells (PSCs) have provided a remarkable increase in solar cell device efficiency [1]. The first report of low-cost DSSCs was published in 1991; many articles have emerged during last twenty years. The starting efficiency was related to DSSC was about 8% which was later improved to over 12%. High efficiency, greater than 12%, was realized using a 10  $\mu\text{m}$  meso-porous  $\text{TiO}_2$  film, sensitized with organic dyes and a cobalt-based redox electrolyte. Solid-state DSSC technology was developed in 1998, in which organic hole-transport material (HTM) was used instead of the liquid electrolyte [2,3]. Low-temperature, solution-process able solar cells have become very attractive because they can be manufactured cost-effectively on large scales with high throughput. Recently, methylammonium lead halide perovskites ( $\text{CH}_3\text{NH}_3\text{PbI}_3$ ) have been identified as promising absorbers for solar cell applications with very impressive power conversion efficiencies (PCEs) of over 15% due to their remarkable long range, their balanced hole and electron transport diffusion lengths and their bipolar charge transport capabilities. [4]

Initial investigations in the area of Perovskite solar cells emerged as an evolution of the DSSC architecture [5]. The development of other types of semi-conducting sensitizers, being in a thin film

or quantum dot (QD) form, enables a reduction in the thickness of the mesoporous TiO<sub>2</sub> layer. Later in 2009, Miyasaka and Coworkers demonstrated the first Perovskite sensitized solar cells using CH<sub>3</sub>NH<sub>3</sub>PbI<sub>3</sub> and CH<sub>3</sub>NH<sub>3</sub>PbBr<sub>3</sub> as light absorbers on TiO<sub>2</sub> layers with halide electrolytes. An efficiency of 3.81% was gotten from CH<sub>3</sub>NH<sub>3</sub>PbI<sub>3</sub> with an observed photocurrent onset from 800 nm approximately. An observed photo-voltage of 0.96 V was obtained from CH<sub>3</sub>NH<sub>3</sub>PbBr<sub>3</sub>, referred to the deeper bromide redox couple, utilized in this kind of solar cells [6].

Organic-inorganic Perovskite solar cells (PSCs), based on CH<sub>3</sub>NH<sub>3</sub>PbX<sub>3</sub> (X = Cl, Br, I), have stood out among various photovoltaic devices due to the superior properties of Perovskite light absorbers, including large visible light absorption coefficients, direct band gap and long diffusion lengths together with the low cost and solution-based fabrication process [7]. Organo-metallic halide Perovskites (e.g., (CH<sub>3</sub>NH<sub>3</sub>) PbI<sub>3</sub>) are considered powerful materials of light absorption. The bandgap energy of such absorbers can be changed by adjusting their inorganic and organic components with overall efficiency ranging from about 3% to 6% [8].

This is aimed at demonstrating the viability of a low-temperature vapor-assisted solution process to construct polycrystalline perovskite thin films with full surface coverage, small surface roughness, and grain size up to micro-scale. Solar cells with as-prepared films attain relatively high power conversion efficiency (PCE) reaching to 12.1%. On the other hand, the presently achieved highest efficiency is based on CH<sub>3</sub>NH<sub>3</sub>PbI<sub>3</sub> using the planar hetero-junction configuration [3]. Heterojunctions have a number of advantages over diffused p-n junction solar cells include a lower junction-formation temperature [17]

One of the main differences between organic and inorganic semiconductors is the presence of tightly bonded excitons (electron-hole pairs). The binding energy of the Frenkel exciton lies in the range from 0.3 to 1 eV. This relatively high binding energy prevents exciton dissociation by an electric field (a non-radiative decay channel). Organic materials have been also widely used for solar cell applications as they have relatively low cost and better flexibility compared with their inorganic counterparts, in addition to their attractive performance characteristics [9].

However, the non-commensurate length scales between absorption length (~100 nm) and the exciton (electron-hole pair) diffusion length (~10 nm) limit the efficiency of Organic Solar Cells (OSCs). Another limitation of extent OSCs is that the maximum solar photon flux occurs near the band edge of organic photoactive materials, where the extinction coefficient is smallest [10]. Current OSCs have attained PCEs of 7-8% by several groups and 12.1% experimentally. Compared to the benchmark of crystalline silicon solar cells, this PCE is still low and must be further improved before OSCs can be marketed in the solar cell market [11].

## BASIC PRINCIPLE

“Perovskites” is the nomenclature for any material that adopts the same crystal structure as calcium titanate, namely, ABX<sub>3</sub>, where A is alkyl-ammonium ions (methylammonium in this work), B is lead ions and X represents halogen ions Cl, Br or I (in this work it is I), Fig.1. Organo-perovskites feature high molar absorption coefficients, though it is, excellent light-harvesting performance for the entire visible range. There are hundreds of different materials that adopt this structure, with a multitude of properties, including insulating, anti-ferromagnetic, piezoelectric, thermoelectric, semi-conducting, conducting, and, probably most famous, superconducting [12].

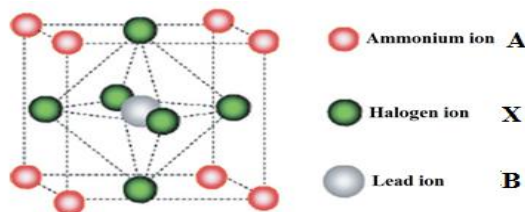


**Figure (1) Unit cell of lead hybrid Perovskite structure  $\text{CH}_3\text{NH}_3\text{PbX}_3$ ,  $\text{ABX}_3$  (methylamine halogen  $\text{MAX}_3$  where X is halogen). [12]**

### Experimental Work

#### A. Deposition of $\text{CH}_3\text{NH}_3\text{PbI}_3$ material (Perovskite growth)

Uniform planar films of methyl ammonium lead tri-iodide  $\text{CH}_3\text{NH}_3\text{PbI}_3$  were first prepared from two materials  $\text{PbI}_2$  and  $\text{CH}_3\text{NH}_3\text{I}$  and then deposited on glass substrates by Aerosol Assisted Chemical Vapor Deposition (AACVD), at  $200^\circ\text{C}$  for 30 minutes with Nitrogen gas as an adjunct throughout the process to ensure a uniform  $\text{CH}_3\text{NH}_3\text{PbI}_3$  film growth speed during the deposition process in University of Missouri's Laboratories. Solution-based techniques have been proposed to fabricate thin films from only one deposition source Fig.2 which is easier and more accurate than the preparation that have been used in other researches where films were fabricated by dual source evaporation, (two deposition technique process), where it is more difficult to control the two materials (organic and inorganic) ratios. The key step is the deposition of Organo-metallic halide Perovskites ( $\text{CH}_3\text{NH}_3$ )  $\text{PbI}_3$  film from one source. The fabricated thickness of  $\text{CH}_3\text{NH}_3\text{PbI}_3$  film was measured by an optical profilometer, to be 200 nm.

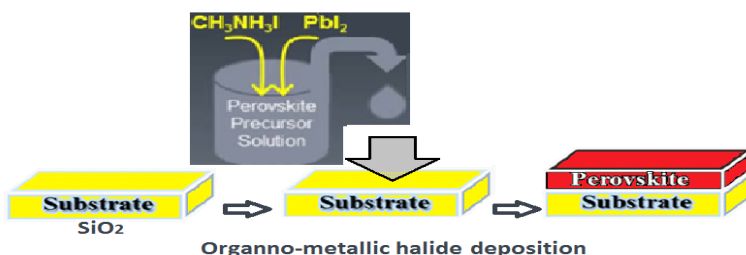


**Figure (2) Schematic illustration of Perovskite Film deposition Vapor-assisted solution process at  $200^\circ\text{C}$  for 30 minutes with Nitrogen gas as an adjunct throughout the process.**

### Deposition

Perovskite material was prepared; the prepared material was deposited on a glass substrate 1 mm thick, instead of deposition on Titanium dioxide substrate, where the base represents the localization region of the charges inside the Perovskite layer generated by the light incident on the solar cell, which will be illustrated in the following preparation procedure.

1. Preparation of Perovskite material: 1.1617g of  $\text{PbI}_2$  and 0.4006g of  $\text{CH}_3\text{NH}_3\text{I}$  are weighed; 15 mL of Di-Methyl Formide (DMF) is obtained using a burette; the DMF is used as catalyst for dissolving the powder mixture. These components are mixed together in a flask and stirred with a magnet bar at  $60^\circ\text{C}$  on a hotplate for 12 hours.

2. 10 ml of  $\text{CH}_3\text{NH}_3\text{PbI}_3$  is diluted using 4.160 ml of Perovskite prepared previously with 5.84 ml of N.N-Di Methyl Formide; both are blended using (Vortex Mixer) for 5 minutes.

3. A deionized water was used to rinse the glass substrates which were then dried using clean air. Uniform planar films of  $\text{CH}_3\text{NH}_3\text{PbI}_3$  were deposited onto glass substrate by Aerosol Assisted

Chemical Vapor Deposition (AACVD), at 200 °C for 30 minutes with Nitrogen gas as an adjunct throughout the process to ensure achieving a uniform speed for film growth of the  $\text{CH}_3\text{NH}_3\text{PbI}_3$  in the deposition process.

### Characterization

In  $\text{CH}_3\text{NH}_3\text{PbI}_3/\text{glass}$  the corresponding X-ray diffraction (XRD) spectra, a three distinct diffraction peaks are noticed at angles 14.10°, 28.44° and 31.80° respectively. These peaks are assigned to the 110, 220 and 310 respectively for the  $\text{CH}_3\text{NH}_3\text{PbI}_3$  crystal which indicate an orthorhombic crystal structure of halide perovskite with high crystallinity [1,13,18]. According to reference [1], there is often a tiny signature peak at 12.65°, corresponding to a low-level impurity of  $\text{PbI}_2$ , appears through perovskite material preparation. The absence of the aforementioned peak in the present perovskite film suggests complete consumption of  $\text{PbI}_2$  via AACVD Vapor deposition mentioned early.

The X-ray diffraction (XRD) patterns of a  $\text{CH}_3\text{NH}_3\text{PbI}_3$  film deposited on glass substrates were recorded (by D/Max- Ultima IV X-ray diffractometer of 3 kW, accelerating voltage of 60 kV); are presented from Rigaku's PDXL thin film X-ray analysis software in Fig.3.

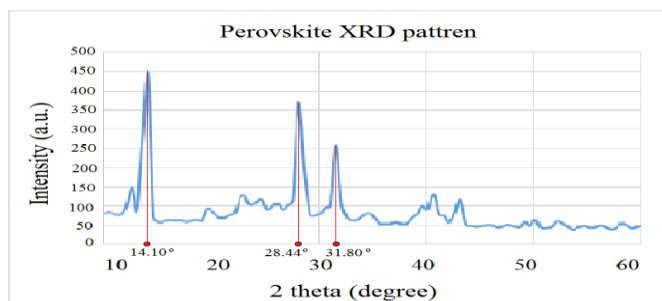


**Figure (3) Intensity against scattering angle for the Perovskite film on glass XRD pattern.**

The perovskite film quality is further evaluated by scanning electron microscopy (SEM) image on the 500 nm scale of the  $\text{CH}_3\text{NH}_3\text{PbI}_3$  film grown onto the glass substrate after the 30 min 200°C, the vapor deposited  $\text{CH}_3\text{NH}_3\text{PbI}_3$  film in Fig.4.(a) shows the characteristics of full surface coverage on the glass substrate, with remarkable grain size up to microscale, grains were observed uniform.

Then a surface roughness of the film was measured by an environmental scanning electron microscope (ESEM), and a top view image of  $\text{CH}_3\text{NH}_3\text{PbI}_3$  film presented in the range of  $5\mu\text{m}\times 5\mu\text{m}$  was calculated to be 23.2 nm, the crystal grains can be observed uniform Fig.4.(b). A typical cross-sectional SEM image indicates the resulting film has a thickness of ~200 nm.

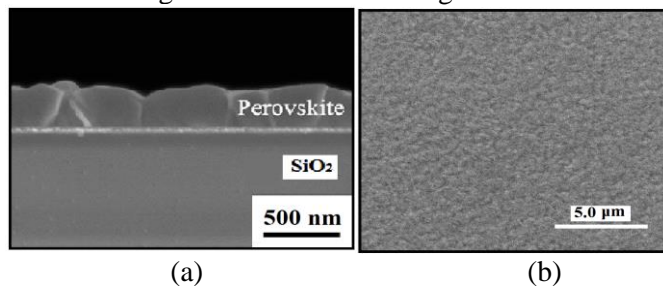


**Figure.4. (a) Cross-sectional SEM image after 30 min 200°C deposition process showing that the vapor deposited  $\text{CH}_3\text{NH}_3\text{PbI}_3$  film is looking uniform on a 500 nm scale. (b) Top view ESEM image of  $\text{CH}_3\text{NH}_3\text{PbI}_3$  appears uniform.**

### UV-Vis

In this work by choosing a one-step planar geometry in fabricating perovskite thin film which can be used subsequently in PV devices. This method is conceptually different from other current solution process that uses two steps depositions. In addition thin film from only one deposition source is easier and more accurate, by avoiding co-deposition of organic and inorganic species. The depositing advantage of perovskite during the in situ growth process provides films with well-defined grain structure and grain sizes up to microscale, then this full surface coverage, and small surface roughness, is suitable for PV applications as shown in Fig.4 (a) and (b).

The thinner samples exhibit inadequate light absorption, especially for long wavelength's range of the light spectrum. In this work it was noticed that by using planar perovskite film, in spite of reducing the thickness of the perovskite layer for solid-state cells to a value less than 2  $\mu\text{m}$ , the solar conversion efficiency was found to be still higher about 15.7 % for thinner samples (those samples that have thickness range with few hundred nanometers).

Using the UV-Vis 2401PC Ultraviolet-Visible Spectrophotometer, absorption spectra were sketched in Fig.5 showing the maximum wavelength to be less than 800 nm ( $\lambda=760$  nm).

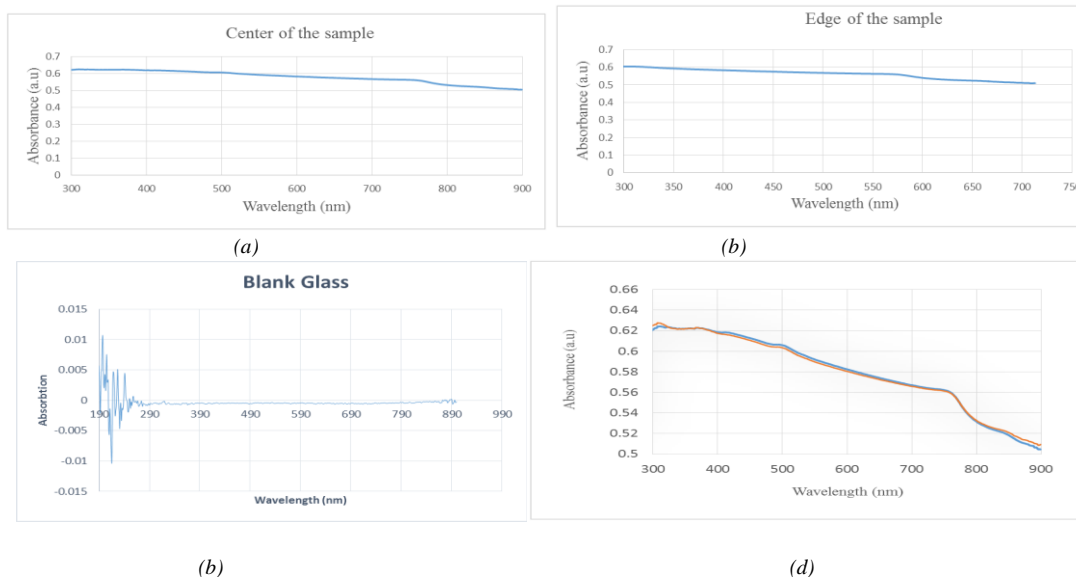


**Figure.5. A typical ultraviolet-visible absorption spectrum of the  $\text{CH}_3\text{NH}_3\text{PbI}_3$  sensitized on a glass film; absorbance was tested (a) at the center and (b) at the edge of the fabricated sample, (c) blank glass as a reference, and the average wavelength  $\lambda$  spectra was calculated to be less than 800 nm (d).**

From Fig.5 (a) it has been pointed out that the  $\lambda_1 \approx 776$  nm absorption peak is attributed to the  $\text{CH}_3\text{NH}_3\text{PbI}_3$  material's direct gap transition from the first valence band maximum to the conduction band minimum, which is approximately 1.63 eV (which corresponds to 776 nm). In Fig.5 (b) the  $\lambda_2 \approx 500$  nm absorption peak is attributed to the transition from lower valence band to the conduction band minimum, which is approximately 2.58 eV (which corresponds to 500 nm), that means the effective region is in the center of the sample.

The bandgap of  $\text{CH}_3\text{NH}_3\text{PbI}_3$  was evaluated to be 1.63 eV from UV photoelectron, UV-vis, and incident photon-to-electron efficiency (IPCE) spectra. [16]. However, a bandgap of around 1.63 eV is enough for absorption wavelength limited to 800 nm Fig.5 (d). Bandgap tuning is required to

extend the absorption to longer wavelengths without sacrificing the absorption coefficient. Replacing perovskite with other organic cations is one approach.

**CALCULATIONS**

*B. Perovskite Energy Bandgap*

The optical bandgap energy ( $E_g$ ) of Perovskite  $\text{CH}_3\text{NH}_3\text{PbI}_3$  was estimated by UV-Vis absorption spectroscopy in addition to its determination from the Tauc plot to be about 1.63 eV.

The Tauc plot is performed according to the following expression [7]:

$$(\alpha h\nu)^m \propto (h\nu - E_g) \dots (1)$$

Where:  $\alpha$  is the absorption coefficient of the material, the quantity  $h\nu$  is the energy of light, and  $m$  is 2 for a direct bandgap semiconductor.

From calculations, the absorbance sketched in Figures 5 and 6 has been used to plot the Tauc plot of Fig.7.

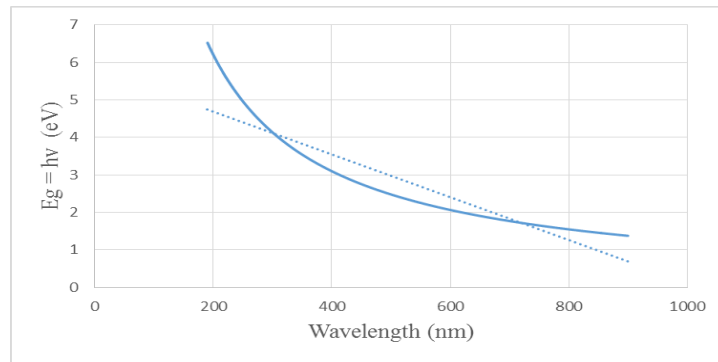


**Figure (6) Perovskite tunable optical bandgap with wavelength.**

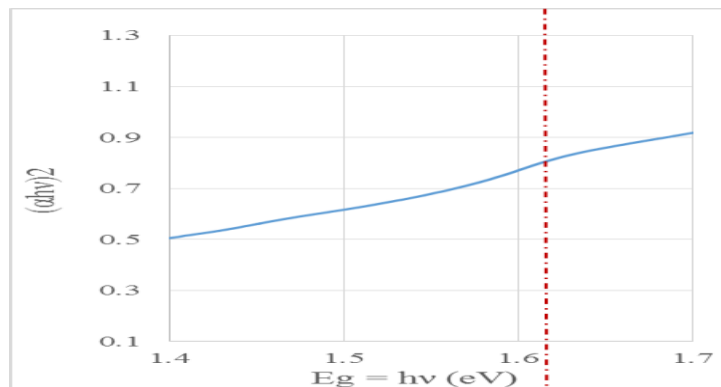


**Figure (7) the optical bandgap ( $E_g$ ) of  $\text{CH}_3\text{NH}_3\text{PbI}_3$  evaluated from the Tauc plot.**

With the aid of the Tauc plot of Fig.7, the bandgap energy is found to be about 1.63 eV, which is sufficient to absorb most light below 800 nm. The absorbance peak is referred to the  $\text{CH}_3\text{NH}_3\text{PbI}_3$  material’s direct gap transition from the first maximum point of the valence band to the minimum point of the conduction band, which is approximately 1.63 eV (corresponding to 760 nm). This

value is consistent with other works for (CH<sub>3</sub>NH<sub>3</sub>)-PbI<sub>3</sub>. For example, Yixin Zhao and Kai [7] carried out a test on CH<sub>3</sub>NH<sub>3</sub>PbI<sub>3</sub> deposited on a 2-μm thick mesoporous TiO<sub>2</sub> film and found a bandgap of 1.53 eV, which is sufficient to absorb most of the light below 600 nm. Besides, Xie Ziang Et. al. [13] performed a test for the CH<sub>3</sub>NH<sub>3</sub>PbI<sub>3</sub> film on a quartz substrate and found a bandgap of 1.59 eV for λ<sub>g</sub> ≈ 779 nm. However, in this work the same Perovskite layer CH<sub>3</sub>NH<sub>3</sub>PbI<sub>3</sub> was deposited using single deposition process which is an easier and cheaper method on a 1-mm glass layer instead of TiO<sub>2</sub> or quartz (see Table 1).

**Table (1) A comparison between different materials used as a substrate with Perovskite.**

material	E <sub>g</sub> (eV)	λ (nm)	thickness (nm)	η (%)	Ref.
glass	1.63	< 800 =760	200	15.7	This work
TiO <sub>2</sub>	1.53	< 600	2000	4.58	[7]
quartz	1.59	< 779	250-500	16.8-23	[12]

**Efficiency**

The absorbance ratio (*A*) can be estimated from the relation:

$$A(\lambda) = 1 - R(\lambda) - T(\lambda) \quad \dots (2)$$

Where: *R* is the reflectance ratio and *T* is the transmittance ratio of the plane-structured CH<sub>3</sub>NH<sub>3</sub>PbI<sub>3</sub> material. The ultimate efficiency *η*, representing the ideal efficiency without taking carrier recombination into account, can be expressed as [14]:

$$\eta = \frac{\int_0^{\lambda_g} I(\lambda) A(\lambda) \frac{\lambda}{\lambda_g} d\lambda}{\int_0^{\infty} I(\lambda) d\lambda} \quad \dots (3)$$

Where: *I*(λ) is the light intensity as a function of wavelength, and λ<sub>g</sub> is the wavelength corresponding to the band gap of the light absorption material.

The solar spectrum and intensity is evaluated according to the AM 1.5 American spectra standard.

Generally, assuming perfect antireflection and perfect light trapping, the absorption spectrum in a thin film with thickness *d* is given by the Yablonoitch limit:

$$A_{\text{Yablonoitch}}(\lambda) = 1 - 1/(4(n(\lambda))^2 \cdot \alpha(\lambda) \cdot d) \quad \dots (4)$$

This limit is only applicable for [*d* > λ/(2*n*(λ))] [15]. The use of CH<sub>3</sub>NH<sub>3</sub>PbI<sub>3</sub> SCs can offer improved efficiency through the fabrication of planar nano textures.

The absorption of the CH<sub>3</sub>NH<sub>3</sub>PbI<sub>3</sub> increases by the increase in film thickness, especially in the long wavelength range of the visible spectrum of light. Although the electron diffusion coefficient depends slightly on the film thickness, the recombination process becomes much faster with thicker films.

In the current work, the thicknesses of the light absorption layers containing CH<sub>3</sub>NH<sub>3</sub>PbI<sub>3</sub> in Perovskite SCs are mostly 200-500 nm. The thickness was measured to be 200 nm and the efficiency was calculated to be 15.7 %.

**Reflection**

Reflection is also an important factor for the SCs. When the solar light is incident normally on the planar material, the reflectivity, *R*<sub>0</sub>(λ), is dependent on both the refractive index *n*(λ) and the extinction coefficient *k*(λ) as described in the following equation:

$$R_0(\lambda) = \frac{[n(\lambda) - 1]^2 + [k(\lambda)]^2}{[n(\lambda) + 1]^2 + [k(\lambda)]^2} \dots (5)$$

Using equation (5), and the acquired  $n(\lambda)$  and  $k(\lambda)$  of the  $\text{CH}_3\text{NH}_3\text{PbI}_3$  material presented in Fig.8 the  $n(\lambda)$  of the  $\text{CH}_3\text{NH}_3\text{PbI}_3$  material lies between those of the inorganic semiconductors and the organics.

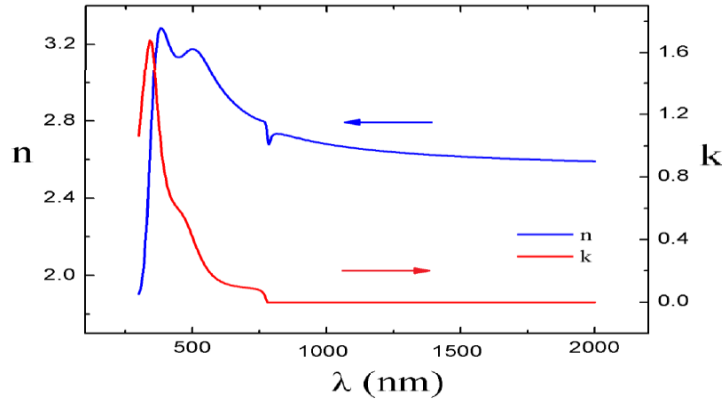


Figure (8)The calculated  $n(\lambda)$  and  $k(\lambda)$  results  $\text{CH}_3\text{NH}_3\text{PbI}_3$  material. [13]

It can be shown that the  $\text{CH}_3\text{NH}_3\text{PbI}_3$  has a small  $R_0(\lambda)$  value of about 2.3. The larger  $k(\lambda)$  and smaller  $n(\lambda)$  of  $\text{CH}_3\text{NH}_3\text{PbI}_3$  illustrates why the Perovskite SC has relatively high efficiency.

**CONCLUSIONS**

As a conclusion, this study has concentrated on  $\text{CH}_3\text{NH}_3\text{PbI}_3$  Perovskite which is used as a light harvester in solid state heterojunction solar cells. Planar thin film nanoparticles (NPs) of Perovskite-structured methyl ammonium lead triiodide  $\text{CH}_3\text{NH}_3\text{PbI}_3$  were produced by one-step process on glass of 1mm thickness. A bandgap was measured about 1.63 eV, which shows sufficient capability in absorbing most light wavelengths lower than 800 nm ( $\lambda = 760$  nm). This article shows an easier and cheaper process for fabricating thin film solar cells than using dual source evaporation for the deposition of Perovskite on  $\text{TiO}_2$  substrate, although Perovskite prepared by two-step coating method shows cuboid-like crystals, which increased absorbing surface area [16]. Reflectance was calculated to be as small as 0.23 that means an improvement in solar efficiency can be achieved in future. Hybrid solar cells, combining inorganic nano-particles and conductive polymer blends are the best developed so far and further improvement is likely to reduce the electricity cost. Recently, the discovery of Perovskite material improves significantly the absorption capacity for their tunable direct bandgap, thus leading to an efficiency boost. A relatively high efficiency of 15.7% has been achieved under the AM 1.5 illumination standard along with excellent long term stability. So, this system may be very attractive for further investigations.

**Acknowledgments**

This work was financially supported by a grant from the Nano technology group in the University of Missouri, Columbia, USA during my sabbatical leave from the University of

Technology, Baghdad. The author sincerely wishes to acknowledge the role of Prof. Shubhra Gangopadhyay, the C.W. LaPierre Endowed Chair Professor in the Electrical and Computer Engineering Department at the University of Missouri and co-director of the MU International Center for Nano/Micro Systems and Nanotechnology, for her valuable discussion and to Dr. Mathai Joseph for his help on the deposition and Perovskite growth mechanism. Also, I thank Assist Prof. Dr. Mutaz Shunasi for his scientific review and help in manuscript language revision.

## REFERENCES

- [1] Qi Chen, Huanping Zhou, Ziruo Hong, Song Luo, Hsin-Sheng Duan, Hsin-Hua Wang, Yongsheng Liu, Gang Li, and Yang Yang, "Planar Heterojunction Perovskite Solar Cells via Vapor-Assisted Solution Process", *J. American Chemical Society*, Nov. 2013.
- [2] Yi Chu Zheng, Shuang Yang, Xiao Chen, Ying Chen, Yu Hou, and Hua Gui Yang, "Thermal-Induced Volmer–Weber Growth Behavior for Planar Heterojunction Perovskites Solar Cells", *Chemistry of materials*, June 2015.
- [3] William H. Nguyen, Colin D. Bailie, Eva L. Unger, and Michael D. McGehee., "Enhancing the Hole-Conductivity of Spiro-OMeTAD without Oxygen or Lithium Salts by Using Spiro(TFSI)<sub>2</sub> in Perovskite and Dye-Sensitized Solar Cells", *J. American Chemical Society*, vol. 136, pp. 10996–11001, July 2014.
- [4] Feng Xian Xie, Di Zhang, Huimin Su, Xingang Ren, Kam Sing Wong, Michael Graetzel, and Wallace C. H. Choy, "Vacuum-Assisted Thermal Annealing of CH<sub>3</sub>NH<sub>3</sub>PbI<sub>3</sub> for Highly Stable and Efficient Perovskite Solar Cells", vol. 9, NO. 1, pp 639–646, Dec. 2015
- [5] Tze Chien Sum and Nripan Mathews, "Advancements in perovskite solar cells: photo physics-behind the photovoltaics", *Energy Environ. Science*, vol. 7, pp. 2518–2534, 2014.
- [6] Nam-Gyu Park, "Organo-metal Perovskite Light Absorbers Toward a 20% Efficiency Low-Cost Solid-State Mesoscopic Solar Cell", *Journal of Physical Chemistry Letters*, vol. 4, pp.2423–2429, July. 2013.
- [7] Jeong-Hyeok Im, In-Hyuk Jang, Norman Pellet, Michael Grätzel and Nam-Gyu Park, "Growth of CH<sub>3</sub>NH<sub>3</sub>PbI<sub>3</sub> cuboids with controlled size for high-efficiency perovskite solar cells", *Nature Nanotechnology*, vol. 9, Nov. 2014.
- [8] Yixin Zhao and Kai Zhu, "Charge Transport and Recombination in Perovskite CH<sub>3</sub>NH<sub>3</sub>PbI<sub>3</sub> Sensitized TiO<sub>2</sub> Solar Cells", *Journal of Physical Chemistry Letters*, vol. 4, pp. 2880–2884, Aug. 2013.
- [9] Gang Li, Rui Zhu and Yang Yang, "Polymer solar cells, nature photonics", *nature photonics*, vol. 6 March, Feb. 2012.
- [10] B. Chen, C. J. Mathai, S. Mukherjee, S. Gangopadhyay, "Indium Tin Oxide Photonic Crystal for Controllable Light Coupling in Solar Cells by an Inexpensive Soft Lithography with HD-DVD and Blu-ray", *ECS Transactions*, vol. 61 (18) pp. 69-82, 2014.
- [11] Minlu Zhang, "Multi-layer Organic Photovoltaic Devices Investigation", Ph.D Thesis, University of Rochester, New York, 2012.
- [12] Bettina V. Lotsch, New Light on an Old Story: Perovskites Go Solar, *Angew. Chem. Int. Ed.*, vol. 53, pp. 635 – 637, Dec. 2014.
- [13] Xie Ziang, Liu Shifeng,<sup>2</sup> Qin Laixiang,<sup>1</sup> Pang Shuping,<sup>3</sup> Wang Wei, Yan Yu, Yao Li, Chen Zhijian, Wang Shufeng, Du Honglin, Yu Minghui, and G. G. Qin, "Refractive Index and Extinction Coefficient of CH<sub>3</sub>NH<sub>3</sub>PbI<sub>3</sub> Studied By Spectroscopic Ellipsometry", *Optical Society of America*, Dec. 2014.

- [14] J.-Y. Chen, "Optical Absorption Enhancement in Solar Cells via 3d Photonic Crystal Structures", *Progress in Electromagnetics Research M*, vol. 17, pp. 1-11, Jan. 2011.
- [15] S. Mokkaapati and K. R. Catchpole, "Nanophotonic light trapping in solar cells", *Journal of Applied Physics* 112, 101101, pp. 1-19, Aug. 2012.
- [16] Hyun Suk Jung and Nam-Gyu Park, "Perovskite Solar Cells: From Materials to Devices", vol.11, no.1, pp. 10–25, *Materials Views, Small journal*, Oct. 2014.
- [17] Heba Salam Tareq, "Deposited Nanostructure Cds Thin Film by Using Pulse Laser Deposition Technique for Fabrication of Heterojunction Solar Cell", *Eng. & Tech. Journal*, Vol.32, Part (B), No.2, 2014.
- [18] Dr.Khaled Z.Yahya and Muhanad Adel Ahmed, "Fabrication and Study Nanostructure Deposited Thin Films Heterojunction Solar Cell", *Eng. & Tech. Journal*, Vol.30, No.1, 2012.